Supporting Information for

Self-crosslinked N-doped Carbon Dots Supported Pd as Efficient Catalyst for Dehydrogenation of Formic Acid at Room Temperature

Zhongxuan Lin[a #], Ouyang Liu[a #], Shuyan Guan[a], Zhao xinru[a], Zhenluo Yuan[a], Xianyun Liu[a, *], Linyan Bian[a], Yanping Fan[a,c], Qiuming Peng[b], Shumin Han[b], Baozhong Liu [a, c, *]

[a]College of Chemistry and Chemical Engineering, Henan Polytechnic University, Jiaozuo, Henan 454003, P. R. China

[b]State Key Laboratory of Metastable Materials Science and Technology, Yanshan University, Qinhuangdao 066004, P.R. China

[c]Henan Key Laboratory of Coal Green Conversion, Henan Polytechnic University, Jiaozuo, Henan 454003, P. R. China

[#] These authors contributed equally to this work.

*** Corresponding Author:** xianyunliu@hpu.edu.cn，HPUliuking@163.com

Computational methods

We have employed the Vienna Ab Initio Package (VASP)[1,2] to perform all the density functional theory (DFT) calculations within the generalized gradient approximation (GGA) using the PBE[3] formulation. We have chosen the projected augmented wave (PAW) potentials[4-6] to describe the ionic cores and take valence electrons into account using a plane wave basis set with a kinetic energy cutoff of 450 eV. Partial occupancies of the Kohn−Sham orbitals were allowed using the Gaussian smearing method and a width of 0.05 eV. The electronic energy was considered self-consistent when the energy change was smaller than 10^{-6} eV. A geometry optimization was considered convergent when the force change was smaller than 0.03 eV/Å. Grimme's DFT-D3 methodology[7] was used to describe the dispersion interactions. The vacuum spacing perpendicular to the plane of the structure is 15 Å. The Brillouin zone integral uses the surfaces structures of 2×2×1 monkhorst pack K point sampling. Finally, the adsorption energies (Eads) are calculated as Eads= Ead/sub -Ead -Esub, where Ead/sub, Ead and Esub are the optimized adsorbate / substrate system, the adsorbate in the structure and the clean substrate respectively. The free energy is calculated as follows:

$$G = E + ZPE - TS$$

where G, E, ZPE and TS are the free energy, total energy from DFT calculations, zero point energy and entropic contributions, respectively.

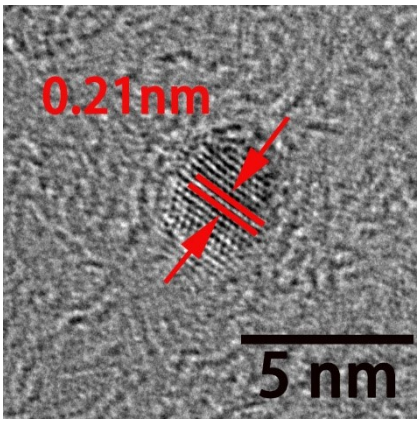

Figure S1 HRTEM images of CE-CDs-III

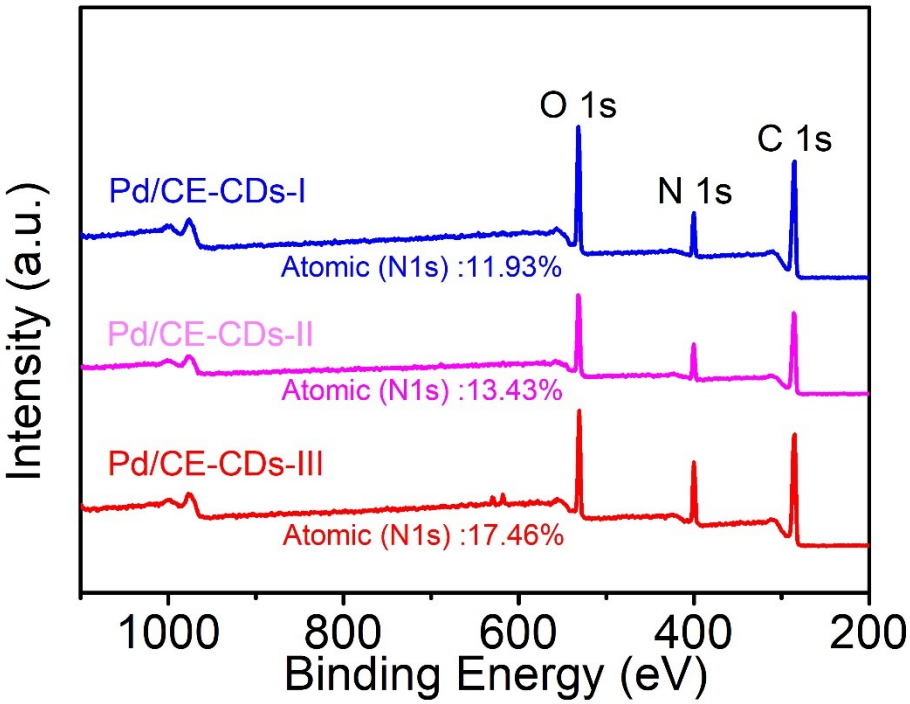

Figure S2 Total spectrum of CE-CDs-X

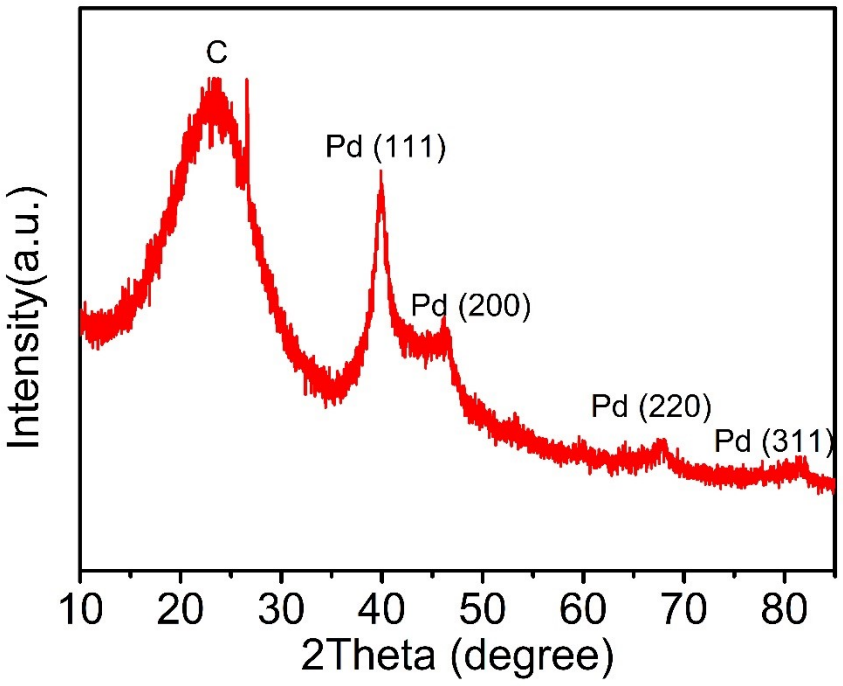

Figure S3 the XRD of Pd/XC-72 sample.

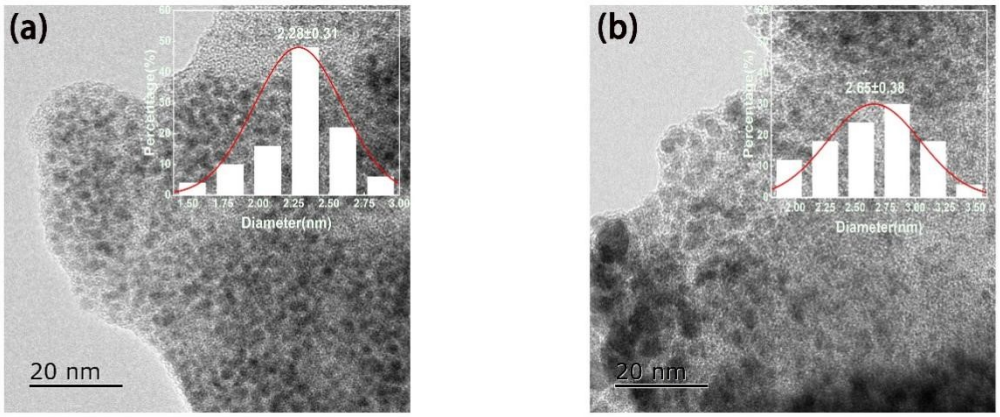

Figure S4 TEM images of Pd/CE-CDs-I (a), Pd/CE-CDs-II (b)

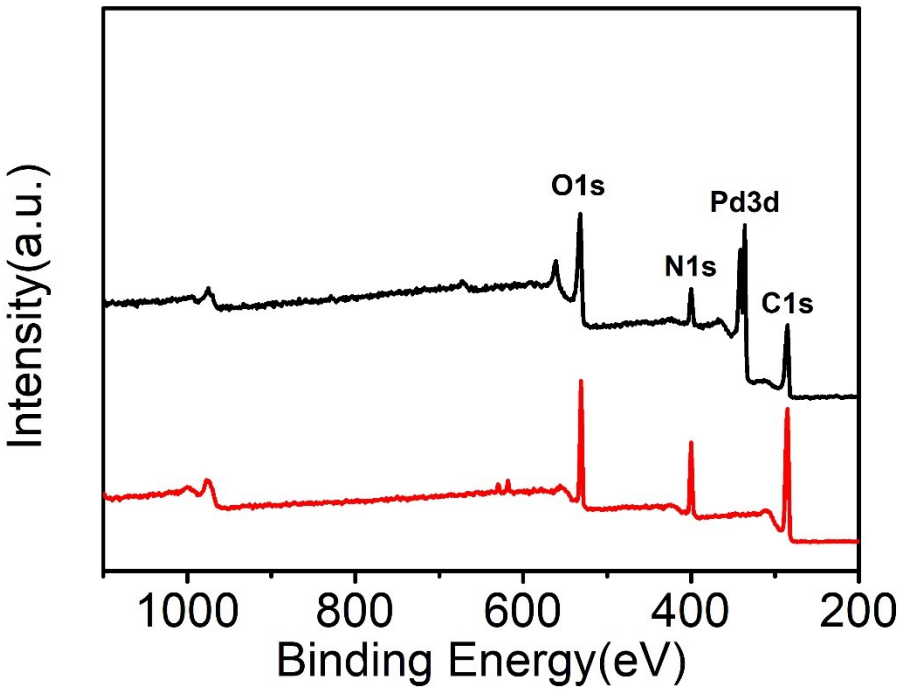

Figure S5 Total spectrum of CE-CDs-III and Pd/CE-CDs-III

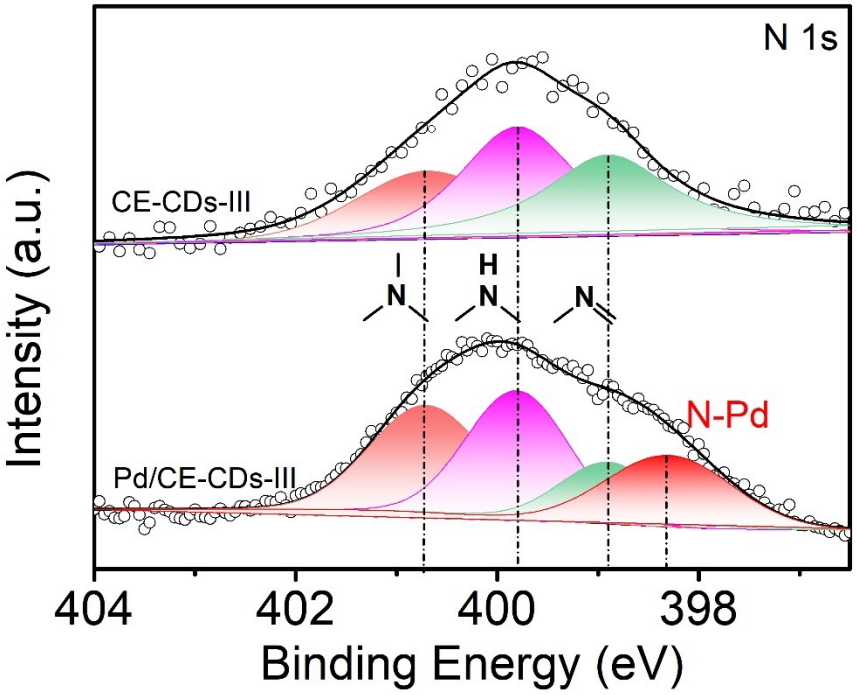

Figure S6 the N 1s peak of CE-CDs-III and Pd/CE-CDs-III

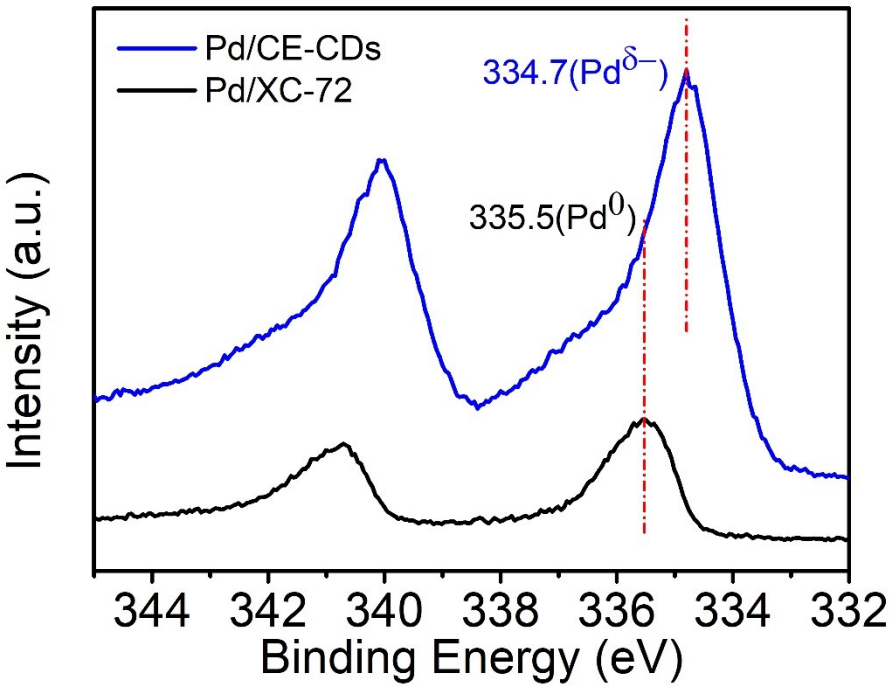

Figure S7 the Pd3d peak of Pd/CE-CDs-III and Pd/XC-72

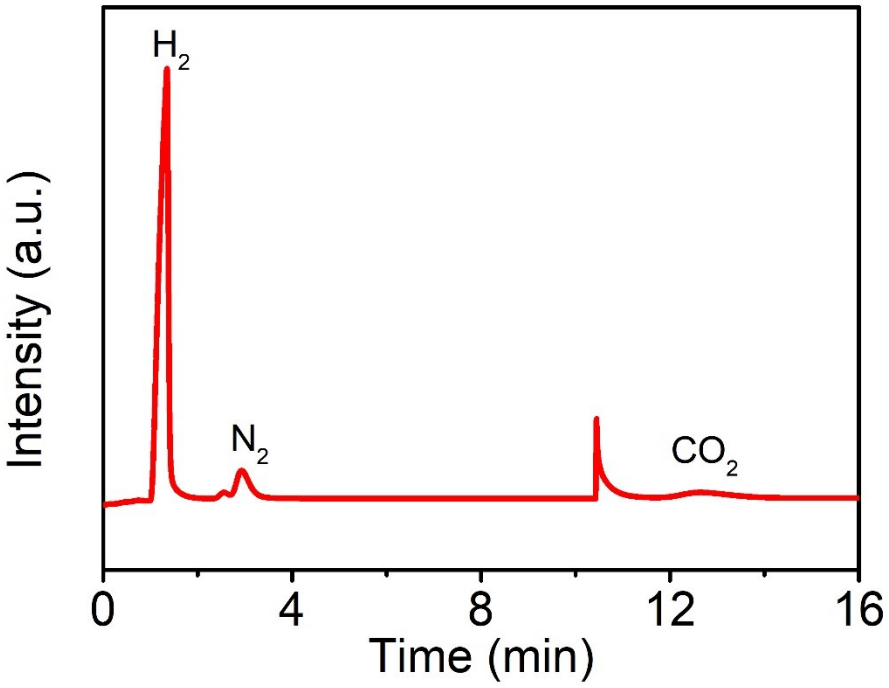

Figure S8 The effluent composition of FA dehydrogenation reaction analyzed by gas chromatography

Table S1: Catalytic activity of various catalysts for FA dehydrogenation (TOF values taken directly from related studies)

Catalyst	Reagent	Temp. (K)	$TOF_{initial}$ (h^{-1})	Average Size(nm)	Ref.
Pd-MnO_X/SiO_2-NH_2	FA	298	140	4.6±1.2	[7]
Pd/C	FA	303	48	1.8-3.5	[8]
PdAu/HPC-NH_2	FA	298	3763	2	[9]
Pd/C	FA	303	6.9	3-4	[10]
Pd/C-$NaBH_4$	FA/SF=11/8	303	304	2.2	[11]
Pd-NH_2/MIL-125	FA/SF=9.8/7.9	305	214	3.1	[12]
Pd/NHPC-NH_2	FA	298	3798	2.5	[13]
Pd@SiO_2	FA/SF=3:1	365	70	20-35	[14]
Pd-N-SiO_2	FA/SF=9/1	358	115	-	[15]
NiPd/NH_2-N-rGO	FA	298	954	10.2	[16]
Pd/MSC-30	FA/SF=1/1	298	750	2.3	[17]
Pd@CN	FA	288	71	2.5	[18]
Methanol mediated Pd NPs/ Vulcan XC-72R	FA/SF=1/1	303	1678	1.4	[19]
Pd@CN900K	FA/SF=1/3	298	1963	1.1±0.2	[20]
Pd/CE-CDs-III	FA	298	256	1.94±0.16	This work

Table S2 The content of Pd and N elements were obtained by XPS.

Sample	Pd content	N content
Pd/CDs-III	7.14%	13.57%
Pd/CDs-III after five tests	7.11%	11.41%

REFERENCES

[1] Kresse, G.; Furthmüller, J. Efficient iterative schemes for Ab initio total-energy calculations using a plane-wave basis set. *Phys. Rev. B* 1996, **54**, 11169-11186.

[2] Perdew, J. P.; Burke, K.; Ernzerhof, M. Generalized gradient approximation made simple. *Phys. Rev. Lett*. 1996, **77**, 3865-3868.

[3] Kresse, G.; Joubert, D. From ultrasoft pseudopotentials to the projector augmented-wave method. *Phys. Rev. B* 1999, **59**, 1758-1775.

[4] Blöchl, P. E. Projector augmented-wave method. *Phys. Rev. B* 1994, **50**, 17953-17979.

[5] Grimme, S.; Antony, J.; Ehrlich, S.; Krieg, H. A consistent and accurate ab initio parametrization of density functional dispersion correction (DFT-D) for the 94 elements H-Pu *J. Chem. Phys.* 2010, **132**, 154104.

[6] Henkelman, G.; Uberuaga, B. P.; Jonsson, H. A climbing image nudged elastic band method for finding saddle points and minimum energy paths. *J. Chem. Phys.* 2000, **113,** 9901-9904.

[7] Bulut, A.; Yurderi, M.; Karatas, Y.; Zahmkiran, M.; Kivrak, H.; Gulcan, M.; Kaya, M. Pd-MnO nanoparticles dispersed on amine-grafted silica: highly efficient nanocatalyst for hydrogen production from additive-free dehydrogenation of formic acid under mild conditions. *Appl. Catal. B* 2015, **164**, 324-333.

[8] Hu, C.; Pulleri, J K.; Ting, S.; Chan, K. Activity of Pd/C for hydrogen generation in aqueous formic acid solution. *Int. J. Hydrogen Energy* 2014, **39** (1), 381-390.

[9] Wang, Z.; Liang, S.; Meng, X.; Mao, S.; Lian, X.; Wang, Y. Ultrasmall PdAu alloy nanoparticles anchored on amine-functionalized hierarchically porous carbon as

additive-free catalysts for highly efficient dehydrogenation of formic acid. *Appl. Catal. B-Environ.* 2021, **291**, 120140.

[10] Wang, X.; Qi, G.-W.; Tan, C.-H.; Li, Y.-P.; Guo, J.; Pang, X.-J.; Zhang, S.-Y. Pd/C nanocatalyst with high turnover frequency for hydrogen generation from the formic acid-formate mixtures. *Int. J. Hydrogen Energy* 2014, **39** (2), 837-843.

[11] Jiang, K.; Xu, K.; Zou, S.; Cai, W.-B. B-Doped Pd catalyst: Boosting room-temperature hydrogen production from formic acid-formate solutions. *J. Am. Chem. Soc.* 2014, **136** (13), 4861-4864.

[12] Martis, M.; Mori, K.; Fujiwara, K,; Ahn, W.-S.; Yamashita, H. Amine-Functionalized MIL-125 with imbedded palladium nanoparticles as an efficient catalyst for dehydrogenation of formic acid at ambient temperature. *The Journal of Physical Chemistry C* 2013, **117** (44), 22805-22810.

[13] Wang, Z.; Wang, C.; Mao, S.; Gong, Y.; Chen, Y.; Wang, Y. Pd nanoparticles anchored on amino-functionalized hierarchically porous carbon for efficient dehydrogenation of formic acid under ambient conditions. *J. Mater. Chem. A* 2019, **7**, 25791-25795.

[14] Yadav, M.; Singh, A.K.; Tsumori, N.; Xu, Q. Palladium silica nanosphere-catalyzed decomposition of formic acid for chemical hydrogen storage. *Journal of Materials Chemistry* 2012, **22** (36), 19146-19150.

[15] Zhao, Y.; Deng, L.; Tang, S.-Y.; Lai, D.-M.; Liao, B.; Fu, Y.; Guo, Q.-X. Selective decomposition of formic acid over immobilized catalysts. *Energy & Fuels* 2011, **25** (8), 3693-3697.

[16] Yan, J.-M.; Li, S.-J.; Yi, S.-S.; Wulan, B.-R.; Zheng,W.-T.; Jiang, Q. Anchoring and Upgrading Ultrafine NiPd on Room-Temperature-Synthesized Bifunctional NH_2-N-rGO toward Low-Cost and Highly Efficient Catalysts for Selective Formic Acid Dehydrogenation. *Adv. Mater.* 2018, **30**, 1703038.

[17] Zhu, Q.-L.; Tsumori, N.; Xu, Q. Sodium hydroxide-assisted growth of uniform Pd nanoparticles on nanoporous carbon MSC-30 for efficient and complete dehydrogenation of formic acid under ambient conditions. *Chemical Science* 2013, **5** (1), 195-199.

[18] Cai, Y.-Y.; Li, X.-H.; Zhang, Y.-N.; Wei, X.; Wang, K.-X.; Chen, J.-S. Highly efficient dehydrogenation of formic acid over a palladium-nanoparticle-based mott–schottky photocatalyst. *Angew. Chem. Int. Ed.* 2013, **52** (45), 11822-11825.

[19] Zhu, Q.-L.; Tsumori, N.; Xu, Q. Immobilizing extremely catalytically active palladium nanoparticles to carbon nanospheres: a weakly-capping growth approach. *J. Am. Chem. Soc.* 2015, **137** (36), 11743-11748.

[20] Wang, Q.; Tsumori, N.; Kitta, M.; Xu, Q. Fast dehydrogenation of formic acid over palladium nanoparticles immobilized in nitrogen-doped hierarchically porous carbon. *ACS Catal.* 2018, **8** (12), 12041-12045.